



*Transactions, SMiRT-26*  
Berlin/Potsdam, Germany, July 10-15, 2022  
Division III

## FUNDAMENTAL STUDY ON HIGH SPEED IMPACT ANALYSIS

**Atsushi Takahashi<sup>1</sup>, Masahito Akimoto<sup>2</sup>,  
Yoshihiko Toda<sup>3</sup>, Kazuki Sato<sup>4</sup>**

<sup>1</sup> Engineer, Engineering Dept., Nuclear Facilities Div., Obayashi Corporation, Japan  
(takahashi.atsushi.ro@obayashi.co.jp)

<sup>2</sup> General Manager, Engineering Dept., Nuclear Facilities Div., Obayashi Corporation, Japan

<sup>3</sup> Researcher, Research Institute of System Technology, JIP Techno Science Corporation, Japan

<sup>4</sup> Engineer, Structural Engineering Division, JIP Techno Science Corporation, Japan

### ABSTRACT

As a fundamental study on the mechanism of shock wave generation, we analyzed this phenomenon of shock waves using an elastic solid Finite Element Method (FEM) that applies the equation of state (EOS) so that sudden changes in pressure can be simulated. In addition, simulation of the penetration test of unreinforced concrete on high speed impact was performed by FEM, and the effect of the EOS and strain rate-dependence on fracture morphology was examined.

In the study of the shock wave, applying the EOS showed the influence of the magnitude of pressure and the waveform shape during impact with high speed. In the simulation of the penetration test of the concrete slab, nonlinear analysis by FEM or Smoothed Particle Hydrodynamics (SPH) method was carried out considering the EOS and strain rate dependence. The bullet penetration and the backside peeling of the concrete slab in the experiment were demonstrated through SPH better than FEM.

### INTRODUCTION

In recent years, the importance of numerical analysis technique that can express penetration and scraping due to impact becomes quite important. In events with high speed impact like an airplane crash and even faster impact like space debris, it is necessary to consider shock waves as well as large deformations of penetration and scraping. However, there are few discussions on shock wave analysis methods in the fields of civil engineering and construction. If the structure does not have enough strength, a special type of failure such as penetration or scraping may occur due to high speed impact. Since the numerical analysis method at high speed impact that causes penetration is in the research phase, conventional empirical formulas are commonly used in structural design.

As a fundamental study on the mechanism of shock wave generation, we analyze this phenomenon of shock waves using an elastic solid FEM that applies the EOS so that sudden changes in pressure can be simulated. In addition, simulation of the penetration test of unreinforced concrete on high speed impact is performed by FEM, and the effect of the EOS and strain rate-dependence on fracture morphology is examined.

## Analysis of Shock Waves by Explicit based FEM Code

During high speed impact, a shock wave is generated due to a sudden change in density, and the pressure rises sharply. In order to simulate this phenomenon in numerical analysis, constitutive laws alone are not sufficient, and the EOS must be introduced. Therefore, in this study, we assume high speed impact with a single bar and examine the effect of considering EOS on the results.

### Equation of State (EOS)

During high speed impact, high pressure compression wave is generated in the object, and it grows and propagates with a discontinuity (shock wave surface) of state quantities (pressure, internal energy and density). The law of conservation of the state quantity before and after the shock wave surface is expressed by the following three equations, called the Rankine-Hugoniot relational equation.

$$\rho_0 u_s = \rho_H (u_s - u_p) \quad (1)$$

$$p_H - p_0 = \rho_0 u_p u_s \quad (2)$$

$$\varepsilon_H - \varepsilon_0 = \frac{1}{2} (p_H + p_0) \left( \frac{1}{\rho_0} - \frac{1}{\rho_H} \right) \quad (3)$$

The symbols correspond to Figure 1 and show the law of conservation of mass, the laws of conservation of mass, momentum and energy, respectively. Introducing the linear relationship between the shock wave velocity  $u_s$  and the particle velocity  $u_p$  in Equation (4),

$$u_s = c_0 + s u_p \quad (4)$$

$$p_H = p_0 + \frac{\rho_0 c_0^2 \eta}{(1-s\eta)^2} \quad (5)$$

$s$  is the material constant,  $\eta = 1 - v/v_0$ . Equation (5) is called the Hugoniot EOS. Furthermore, since the internal energy dependence of pressure cannot be ignored under high pressure, the Mie-Grüneisen type EOS is introduced.

$$p = p_c + \frac{\Gamma}{v} \cdot (\varepsilon - \varepsilon_c) \quad (6)$$

$p_c$ : pressure due to volume dependence,  $\varepsilon_c$ : internal energy due to volume dependence,  $v$ : relative volume ( $= 1/\rho$ ),  $\Gamma$ : Grüneisen coefficient. Adopting Hugoniot EOS for the volume-dependent term leads to the following Mie-Grüneisen-Hugoniot EOS.

$$p = p_H + \frac{\Gamma}{v} \cdot (\varepsilon - \varepsilon_H) \quad (7)$$

By introducing Equation (7), the commercial code can handle shock waves that reflect Equations (1) to (6). Since high-speed impact is a momentary phenomenon, it is often solved under adiabatic conditions (isentropic conditions).

Therefore, the isentropic curve of the EOS is obtained from Equation (7). The adiabatic condition is expressed by the following equation.

$$p dv + d\varepsilon = 0 \quad (8)$$

According to Menikoff, the isentropic condition is expressed by the following relational expression that combines equations (7) and (8).

$$\frac{d}{dv} \left( \frac{\varepsilon}{\phi} \right) = \frac{\left( p_H - \frac{\Gamma}{v} \varepsilon_H \right)}{\phi} \quad (9)$$

$\phi$  is a coefficient that represents the change in internal energy due to volume change, and is expressed by the following formula.

$$\phi(v) = \exp \left[ - \int_{v_0}^v \left( \frac{\Gamma(v')}{v'} \right) dv' \right] = -e^{-g_0(v-v_0)} \quad (10)$$

It is assumed that  $\Gamma(v')/v' = \Gamma_0/v_0 = g_0$ . Equation (9) can be integrated for volume  $v$  to obtain the following relational equation for internal energy.

$$\varepsilon = \phi(v) \int_{v_0}^v -\phi(v)^{-1} \{ p_H - g_0 \varepsilon_H \} dv' \quad (11)$$

By substituting Equation (11) into Equation (7), the relational expression between pressure and relative volume under isentropic conditions can be obtained.

$$p = (p_H - g_0 \varepsilon_H) - g_0 \phi(v) \int_{v_0}^v -\phi(v)^{-1} \{ p_H - g_0 \varepsilon_H \} dv' \quad (12)$$

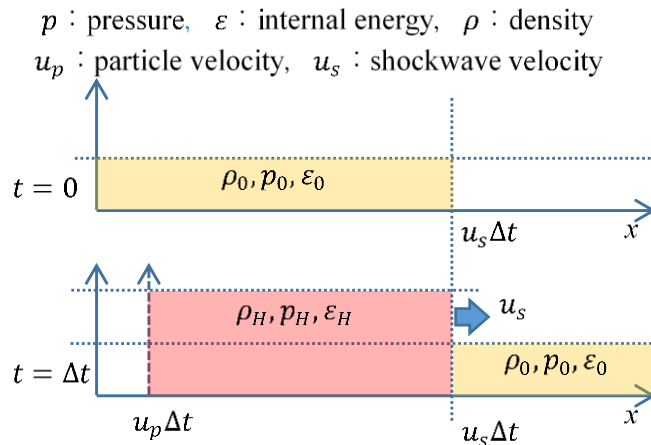


Figure 1. State quantities before and after the shock wave surface

### Shock Wave Analysis by FEM

The analytical model is uniaxial state elastic bar of one side length 0.05 (m) square and 0.5 (m) length as shown in Figure 2. A forced velocity is loaded at one end of the bar, and the opposite end is assumed to be a non-reflective boundary. The material is assumed to be Stainless steel (SUS304). Material properties are shown in Table 1. The program used for the analysis is LS-DYNA10.2.

Figure 3 shows a contour plot of density and internal energy. It can be seen that the Rankine-Hugoniot relationship can be used to represent the discontinuity surface (shock wave surface) of the state quantity.

Figure 4 shows the pressure time history at the center of the member ( $x=250$  (mm)). With a loading velocity of 100 (m/s), there is little effect on the EOS, but with loading velocities of 1,000 (m/s) and 10,000 (m/s), there are significant differences in the size, shape, and propagation velocity of the pressure wave. Figure 5 shows the stress propagation for the 10,000 (m/s) case. The pressure wave changes from smoothed mountain-shaped to sharp triangular in the time domain. This might be caused by overlapped pressure just

like the Doppler effect for moving sound source (loading surface). Introducing the EOS could lead such shift with varying propagation velocity which depends on the pressure.

The  $p - v$  relationship at a loading velocity of 10,000 (m/s) (with EOS) is consistent with the theoretical solution of equation (12) (Figure 6).

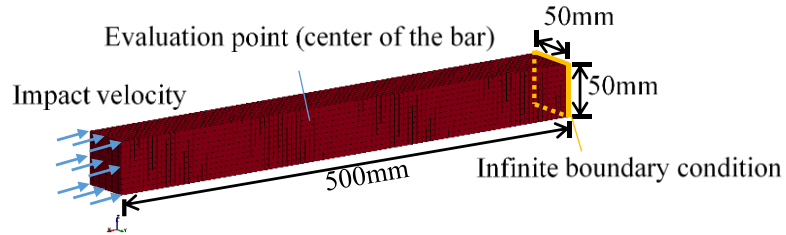


Figure 2. Analysis Model

Table 1. Material Property

Item				Stainless
Material property parameters	Elastic modulus	$E$	N/mm <sup>2</sup>	$2.0 \times 10^5$
	Velocity of longitudinal elastic wave	$Vp$	m/s	5838
	Poisson's ratio	$\nu$	-	0.3
	Density	$\rho$	kg/m <sup>3</sup>	7900
EOS parameters	Bulk speed of sound	$c$	m/s	4570
	S-value	$S$	-	1.49
	Grüneisen coefficient	$\Gamma$	-	2.17

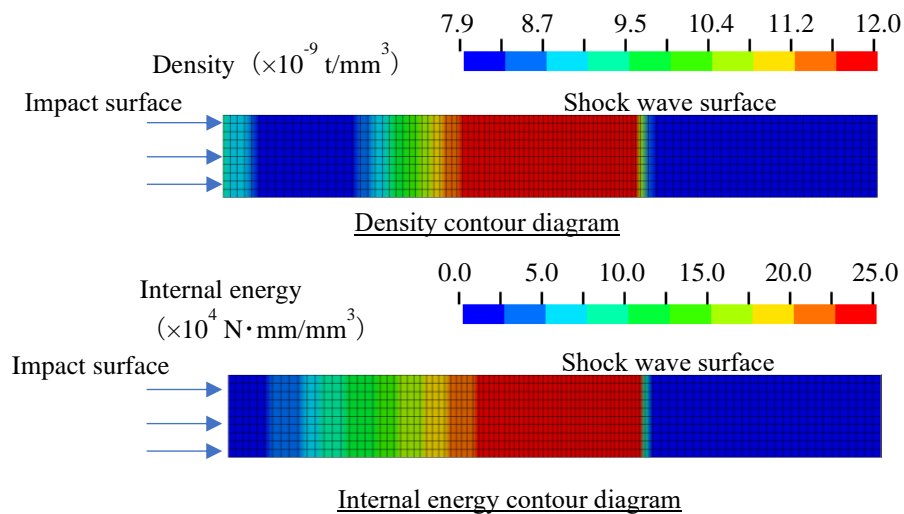


Figure 3. State quantity contour diagram

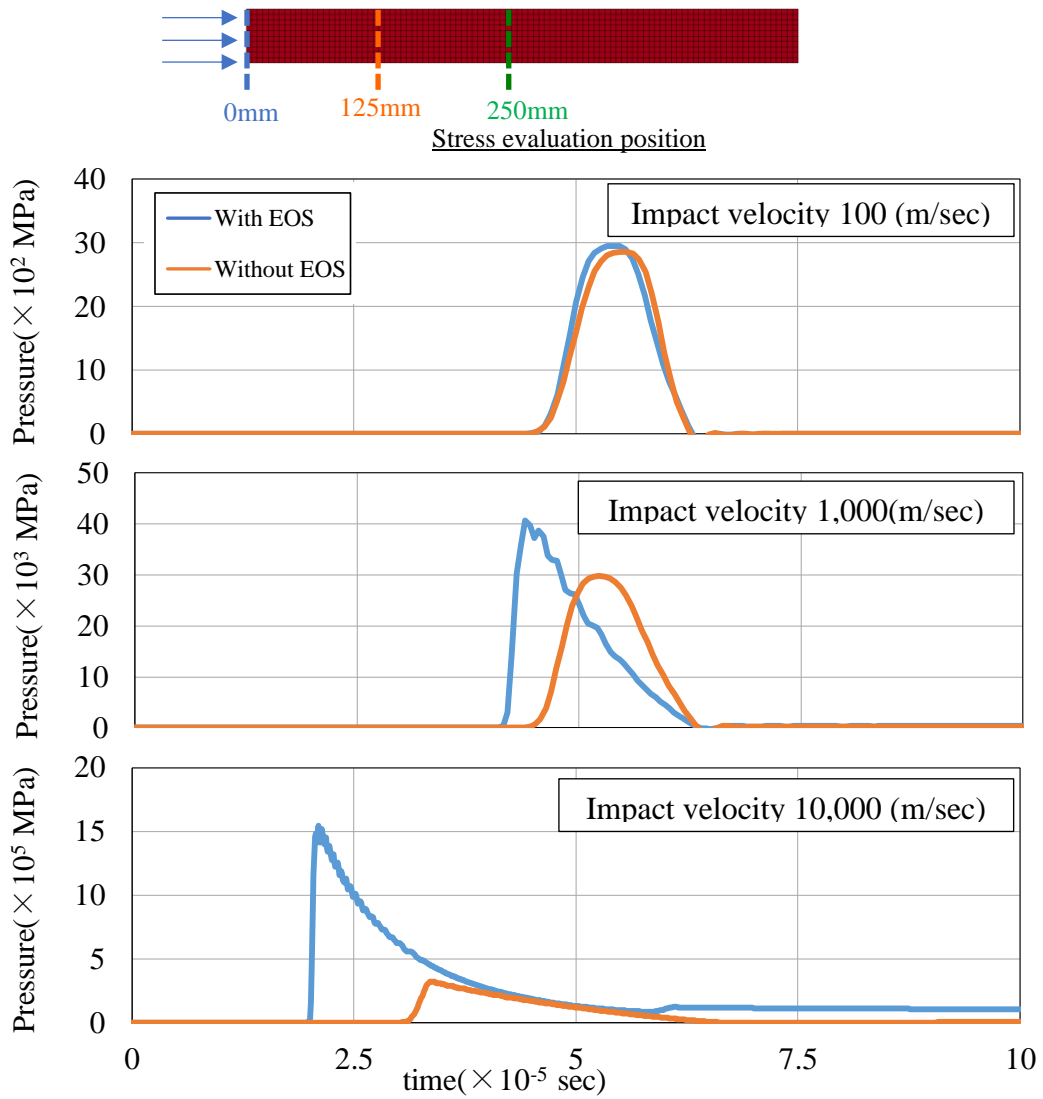


Figure 4. Pressure time history ( $x=250$ )

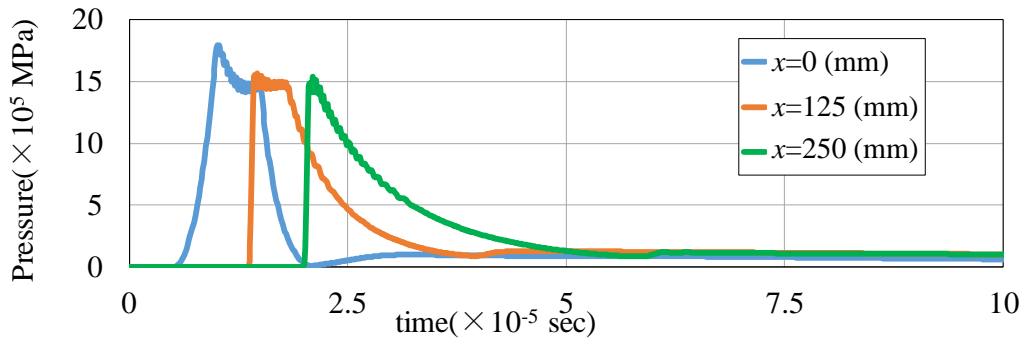


Figure 5. Pressure time history (Impact velocity:10,000 (m/s), With EOS)

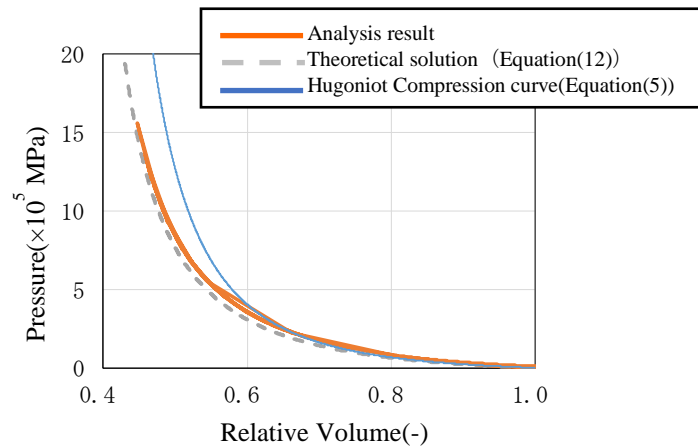


Figure 6. Pressure – Relative Volume ( $p$ - $v$ ) Relation (Impact Velocity:10,000 (m/s), With EOS)

### Simulation of The Penetration Test of Unreinforced Concrete slab

As a fundamental study on high speed impact analysis with penetration, simulation of the penetration test of unreinforced concrete slab is performed by FEM, and the effect of the EOS and strain rate-dependence on fracture morphology is examined. SPH method is used to improve the accuracy of reproducing the penetration velocity of bullet.

#### Outline of The Penetration Test

The simulation is based on an experiment by Hansson (2011) in which a bullet impacted an unreinforced concrete slab. The target of the impact was a circular concrete plate wrapped with an 8 mm thick steel plate, as shown in Figure 7 (left). The bullet had a chromium-nickel-molybdenum steel shell with an Ogive-type warhead and was mass-adjusted with cementitious materials. Two cases of experiments with different bullet incidence angles are analyzed. Table 2 shows the test conditions and results for each experimental case. Figure 7 (right) shows a photograph taken after the experiment in the vertical case. Crater-like shear failure surfaces can be observed on both the front and back surfaces.

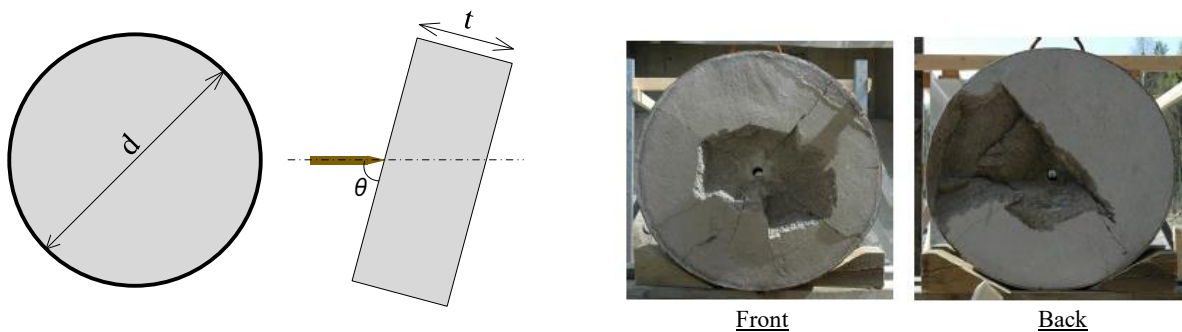


Figure 7. Specimen shape(left) and Experimental results of vertical case(right)

Table 2. Specimen parameters and experimental results

	Case	Vertical	Oblique
Impact condition	Angle $\theta(^{\circ})$	90	60
	Velocity $v(\text{m/sec})$	420	
Concrete slab	Diameter $d(\text{mm})$	1200	1500
	Thickness $t(\text{mm})$	600	540
	Thickness of Steel plate (mm)	8	
	Compressive strength (MPa)	54.8	
	Elastic module (GPa)	31.3	
	Density ( $\text{kg/m}^3$ )	$2.31 \times 10^3$	
	Bullet	Length (mm)	450
Diameter (mm)		50	
Mass (kg)		4.5	
Shape		CRH8.0	
Elastic module (GPa)		212.7	
Experimental Result	Penetration velocity (m/sec)	139	8*
	Front crater diameter (mm)	650	775*
*Average of two result	Front crater depth (mm)	110	235*
	Back crater diameter (mm)	900	1050*
	Back crater depth (mm)	155	200*

### *Parametric Study for Vertical Impact Cases*

The analysis software used is LS-DYNA 10.2. First, parametric study is conducted for the vertical case with concrete strength as a parameter. Concrete and bullets are modeled with solid elements, and steel plates are modeled with shell elements. In order to consider the consolidation phenomenon under high pressure, we use Riedel-Hiermaier-Thomas (RHT) model that can consider the EOS assuming the adiabatic process and simulate the experimental results by considering the strain rate dependency. Bullets and steel plates are assumed to be elastic. Referring to an example of analysis of impact of a rigid flying object on a concrete slab by Beppu et al. (2007), four cases of analysis were conducted, in which the compressive and tensile strengths. The RHT model takes into account increasing rates of those strengths which depend on the strain rate shown in Table 3.

The slope of the yield surface up to uniaxial compressive strength is determined to be consistent with the Drucker-Prager constitutive law (linear model). The tensile yield surface is determined so that the intersection with the hydrostatic axis coincides with the negative pressure limit of Beppu et al. Figure 8 compares the yield surfaces of the RHT model we set up with those of Beppu et al. Erosion strain is assumed to be 250% equivalent strain. Based on the experimental borehole shape, the effect of friction is assumed to be enough small, and not to be considered in this analysis

Figure 9 shows the results of the analysis with the increase factor as a parameter. In the experiment, push-through shear failure is observed on the back side of the concrete slab. When strength of concrete is increased to account for the strain rate, the shear failure line on the back side became clear, and a shear failure line equivalent to that in the experiment is obtained at a strain rate of 10 (1/s). This result is equivalent to that of Beppu et al. However, no craters on the front side are represented in either case.

### Simulation Analysis of Oblique Impact Case

The analysis results for the oblique impact case are shown in Figure 10. These are the result of the strength for the strain rate of 10 (1/s), which is the closest to the experimental results in terms of failure morphology. As in the vertical impact case, the fracture morphology was generally equivalent to that of the experiment.

### Analysis Results for SPH Model

The FEM study shows that the penetration velocity is different from the experiment. The SPH method is considered suitable for expressing the penetration velocity because it can rationally express delamination. Therefore, a simulation analysis using the SPH method is conducted. All material constants are assumed to be the same as in the FEM model. An increase factor of dynamic strength equivalent to a strain rate of 10 (1/s, shown in Table 3) are considered for compressive and tensile strength of concrete.

A comparison of maximum shear strain contour plots at the end is shown in Figure 11. The FEM results show that the bullet stop inside the concrete slab and does not penetrate. However, the results of the SPH method is able to represent the penetration of the bullet, and SPH particles are detached from both front and back surfaces, resulting in a crater-like fracture morphology. Figure 12 shows the time history of bullet velocity. The results of the SPH method shows that the bullet velocity remained above 100 m/sec, which is comparable to the experimental results. Therefore, it is confirmed that the SPH method can simulate penetration phenomena that are difficult to be represented by FEM.

Table 3. Increase factor of Dynamic Strength

Strain rate(1/s)	Increase factor of compressive strength	Increase factor of tensile strength
Static	1.00	1.00
10 <sup>-1</sup>	1.25	1.70
10 <sup>0</sup>	1.43	2.44
10 <sup>1</sup>	1.69	4.05

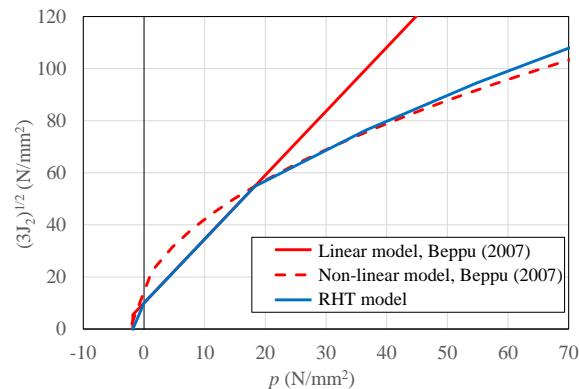


Figure 8. Comparison of yield surfaces (compression is positive)

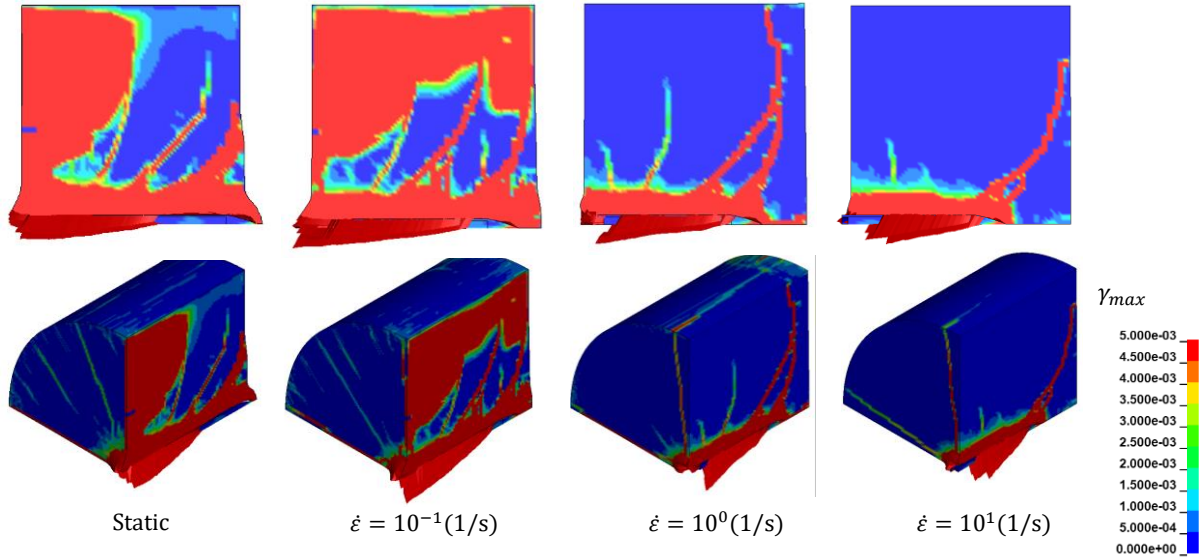


Figure 9. Maximum shear strain contour diagram of vertical impact case

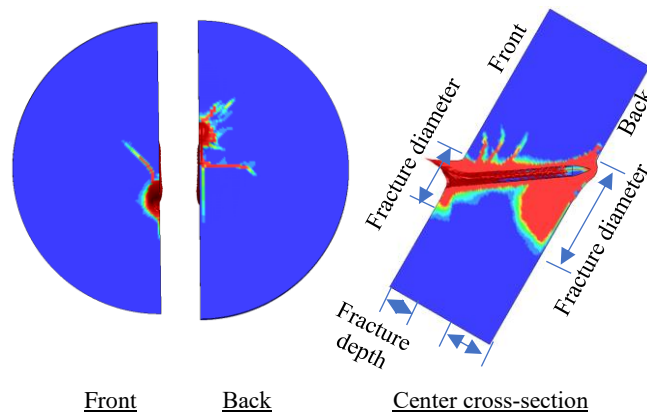


Figure 10. Maximum shear strain contour diagram of oblique impact case

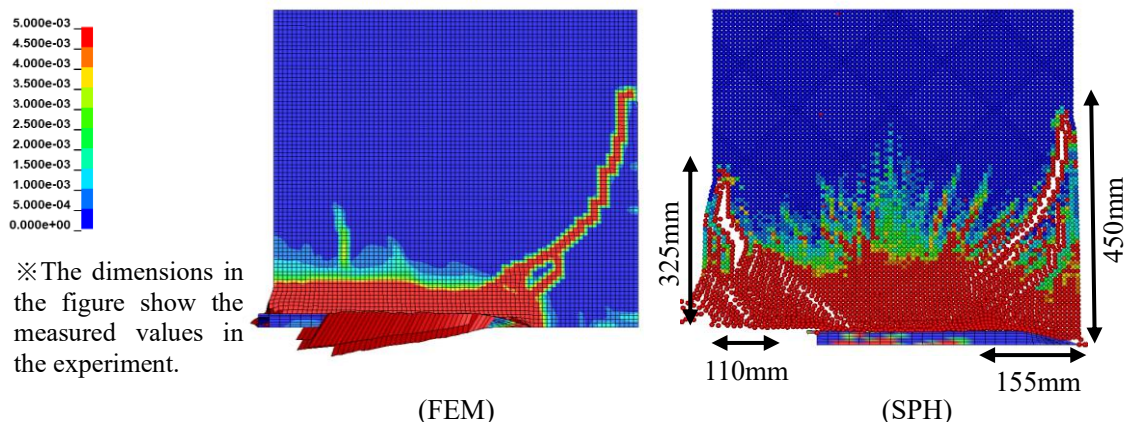


Figure 11. Comparison of maximum shear strain contour diagrams

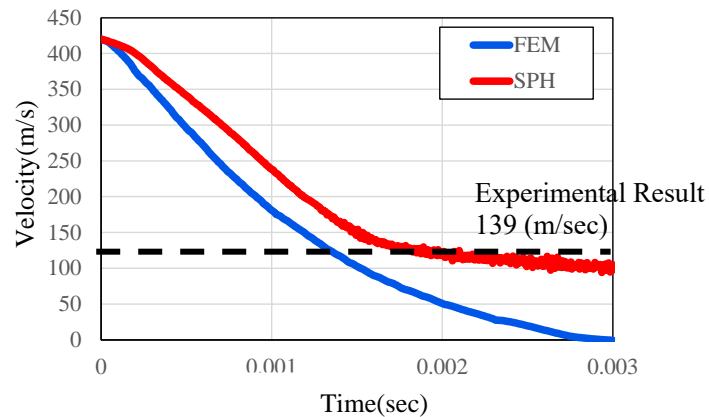


Figure 12. Velocity time history of the bullet

## CONCLUSION

As a fundamental study on high-speed impact, the existing experiment was analytically simulated focusing on shock waves.

First, the impact velocity and the effect of the EOS on the results were examined for the uniaxial state elastic bar model. It was confirmed that when EOS was introduced, the pressure and propagation velocity under high-speed loading became larger. Furthermore, the pressure wave changes from smoothed mountain-shaped to sharp triangular in the time domain. Therefore, it is considered that the introduction of EOS is necessary for the high-speed impact problem.

Next, a simulation analysis of the penetration test of unreinforced concrete slab was performed. By considering a strain rate of 10(1/s) and EOS, a shear failure equivalent to that of the experiment was obtained on the back side. Since the penetration velocity was different from the experiment in the FEM analysis, the SPH method was used to study the penetration velocity. As a result, it was confirmed that the SPH method can reproduce the penetration velocity. By selecting a numerical analysis method that satisfies the energy conservation law, it was confirmed that the penetration phenomenon, which is difficult to be represented by FEM, can be simulated more rationally.

## REFERENCE

Håkan Hansson (2011): *Warhead penetration in concrete protective structures*, Licentiate Thesis of KTH Royal Institute of Technology.

Menikoff (2016): *Complete Mie-Gruneisen Equation of State*, Los Alamos National Lab.

Takashi Matsushima, Keiko Watanabe (2013): *High speed projectile impact to sand deposit: Soil mechanics interpretation of Hugoniot equation of state* (in Japanese), JSCE A2, Vol.69, No.2(Vol. 16), pp. I\_371-I\_378.

Masuhiro Beppu, Koji Miwa, Masaharu Itoh, Masahide Katayama, Tomonori Ohno (2007): *A numerical study on mechanism of the local damage of concrete plate subjected to impact by rigid projectile* (in Japanese), Journal of structural engineering, Vol.53A, pp. 1293-1304